Tight focusing and blue shifting of millijoule femtosecond pulses from a conical axicon amplifier

William M. Wood, Glenn Focht, and M. C. Downer

Physics Department, University of Texas at Austin, Austin, Texas 78712

Received June 7, 1988; accepted August 11, 1988

We focus millijoule femtosecond pulses to a spot radius of 2 μm after amplification free of phase-front distortion in a Nd:YAG-pumped conical axicon dye cell. Peak focal intensities reach 10^{16} W/cm^2, creating an intense spark that is caused by air breakdown at the focus. Intensity-dependent blue shifts of the pulse spectrum as large as 11 nm are observed as a result of temporally asymmetric self-phase modulation in the air-breakdown plasma.

Amplification of femtosecond pulses to millijoule and higher energies has opened up the study of the interaction of matter with radiation fields of unprecedented intensity.[1] While the highest femtosecond pulse energies have been reached in the ultraviolet using excimer amplifiers,[2] high-power dye amplifiers pumped by Nd:YAG[3,4] or excimer[5–7] pump lasers remain an attractive alternative for generating millijoule femtosecond pulses at visible wavelengths because of their lower cost and the ease of suppressing amplified spontaneous emission with common fast saturable absorber dyes.[8] On the other hand, the output of such amplifiers often suffers from poor transverse beam quality and limited focusability caused by severe phase-front distortion during the amplification process. We have constructed a high-power dye amplifier pumped by a Q-switched Nd:YAG laser with a doughnut-mode output that achieves near-diffraction-limited focusing of 100-fsec millijoule pulses without any spatial filtering. The peak intensity at our tightest focus (~2-μm radius) reaches 10^{16} W/cm^2, where breakdown of air at atmospheric pressure is easily observed. This focusability equals that reported for lower-power, higher-repetition-rate amplifiers.[9]

Critical to achieving this result has been a final-stage gain cell of conical axicon geometry.[10–12] All high-power femtosecond dye amplifiers have faced the dual challenge of achieving high gain while maintaining a large output beam diameter (~1 cm) to avoid nonlinear optical effects near the end of the amplification process, making preservation of good beam quality difficult. A well-known and widely replicated system uses longitudinal pumping with counterpropagating pump and signal pulses.[3] However, in this geometry pump pulses impress their often poor beam quality on the femtosecond pulse, thus sacrificing focusability. Recently, improved beam quality and focusability have been reported[4,5,7] with amplifiers using transversely pumped prismatic Bethune cells.[13] Such cells, while well matched to the rectangular profile of excimer laser pulses,[5] are poorly matched to circular Nd:YAG pulses. Axicon cells, on the other hand, ideally match doughnut-mode Nd:YAG pulses, since the weak central portion of the pump is blocked. Moreover, axicons provide other unique advantages over Bethune cells that arise from the radial incidence of the pump into the gain region,[10,11] e.g., maximum gain at the center of the pulse profile and superior pumping efficiency. Kühnle *et al.*[11] have recently demonstrated these features quantitatively using small axicon cells (gain region ~2 cm long) to amplify nanosecond pulses of small diameter (~2.5 mm).

We have scaled the beam diameter and axicon cell to the fourfold-larger size required for amplifying femtosecond pulses to millijoule energy. Figure 1(a) shows

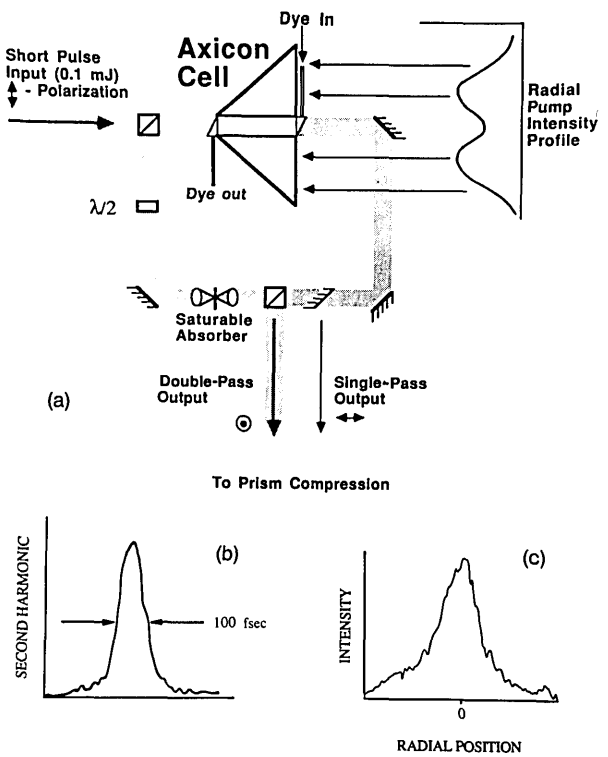

Fig. 1. (a) Final-stage geometry for the femtosecond axicon dye cell amplifier. (b) Autocorrelation trace of pulses amplified to 1 mJ in the axicon system after pulse compression with a prism pair. A sech^2 pulse profile was assumed in arriving at the pulse duration shown. (c) Cross-sectional profile of an unfocused output beam from axicon cell, averaged over 100 shots, measured by expanding the beam onto a diode array.

0146-9592/88/110984-03$2.00/0

the final (fourth) stage of our amplifier. The first three stages (not shown) use standard transversely pumped gain cells to preamplify femtosecond pulses from a colliding-pulse mode-locked laser to 0.1 mJ at a 10-Hz repetition rate. These pulses are then expanded to 1-cm diameter and injected into the gain region of the axicon, an 8-cm-long cylindrical flow tube containing $\sim 5 \times 10^{-5}$ M Rhodamine 640 centered on the axis of a solid glass cone. Incident to the base of the cone and expanded to match its 8-cm radius, counterpropagating 220-mJ 532-nm pump pulses internally reflect from the sides and enter the gain medium at exact radial incidence. Output is extracted after a single pass for ~0.6 mJ/pulse or returned for a second pass through suitable polarizing optics and a saturable absorber as shown for ~1.3 mJ/pulse. Dispersively broadened output pulses are then compressed to 100 fsec with a pair of Brewster-angle SF10 prisms[14] [see Fig. 1(b)] without diminishing pulse energy. Figure 1(c) shows the nearly Gaussian cross-sectional intensity profile of the unfocused output beam.

Figure 2(a) shows for the first time to our knowledge the tight focusability of millijoule femtosecond pulses amplified in a conical axicon cell. These measurements show transmission of the beam focused at $f/2$ by a 7× microscope objective through a 3-μm-diameter pinhole translated in 1-μm steps across the beam waist, with the beam attenuated to avoid damaging the pinhole. The bottom trace shows the focused profile of our unamplified colliding-pulse mode-locked beam after passage through the unpumped amplifier with the saturable absorbers removed. After deconvolving the pinhole diameter, we find a spot radius of only 1.5 μm, close to the diffraction limit. The middle trace shows the profile after preamplification in the first three stages. The spot radius has now increased to 2.3 μm. Finally, the upper trace shows the profile after amplification to 0.6 mJ in the axicon, before the compressor. The focal radius is still 2.3 μm, corresponding to a peak intensity of 0.7×10^{16} W/cm^2 for the dispersively broadened 600-fsec pulses emerging from the axicon. The axicon cell preserves focusability perfectly. Focal radii were confirmed by measuring fractional power transmission through the pinhole. After compression the focal radius increases slightly (to 3 or 4 μm), probably because of the poor surface flatness (~2λ) of our prisms over the large beam area (~1.5 cm^2) needed to avoid self-phase modulation in the highly nonlinear SF10 glass. For the compressed pulse at maximum intensity in air we measured focal radii of 4–5 μm by analyzing damage spot profiles on silicon.[15] Hence nonlinear processes affect focal spot size only slightly at high intensity. Autocorrelation traces after $f/2$ focusing and recollimation over the full range of pulse energies show less than 10% temporal broadening from dispersion in the glass optics or from the air-breakdown process described below. We thus conclude that our focused 100-fsec pulses reach a peak intensity of 10^{16} W/cm^2 at their maximum energy.

As an application of the tight focusing capability of our amplifier system we have studied the interaction of tightly focused millijoule femtosecond pulses with air. At gas pressures up to 40 atm and light intensities up to several 10^{13} W/cm^2, other groups have observed

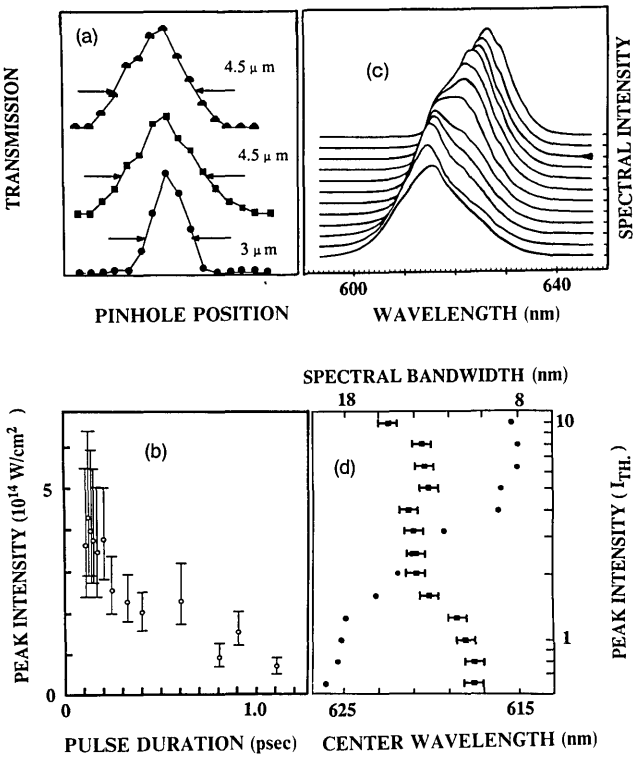

Fig. 2. (a) Focused beam-waist profile of an unamplified colliding-pulse mode-locked laser output (bottom curve), after preamplification to 0.1 mJ before the axicon gain cell (middle curve), and after amplification to 0.6 mJ in the axicon cell (top curve). Data points show intensity transmitted through a 3-μm pinhole translated in 1-μm steps across the focal plane of a 7× microscope objective. (b) Breakdown threshold intensity for air as a function of pulse duration. (c) Spectra of 100-fsec millijoule pulses transmitted through air-breakdown spark, with focal intensity increasing toward the front in increments of 0.1 optical density. The arrow denotes the breakdown threshold. Successive curves have been displaced from each other in an exact vertical direction for ease of presentation. Note the blue shift as intensity increases and the saturation of the blue shift above 2×10^{15} W/cm^2. (d) Variation of center wavelength (circles) and spectral bandwidth (FWHM, squares with error bars) of the spectra shown in (c), with peak intensity in units of threshold breakdown intensity.

supercontinuum generation.[16] Furthermore, in atmospheric air Kühlke *et al.*[17] have observed spectral broadening of unfocused or loosely focused femtosecond pulses, with no visual evidence of air breakdown. However, with our tighter focus ($f/2$), shorter confocal beam parameter ($z_0 \sim 100$ μm), and higher peak intensity (10^{14}–10^{16} W/cm^2), we observe markedly different effects. At a sharply defined threshold we observe air breakdown, as manifested by intense light emission from the plasma formed at the focus. Figure 2(b) shows that the threshold breakdown intensity in air (as determined by appearance of a spark visible to the dark-adapted eye) is a strong function of pulse duration, which was varied by adjusting the prism compressor. The trend of decreasing threshold with increasing pulse width agrees qualitatively with avalanche ionization models of gas breakdown at longer pulse durations.[18] Indeed, direct multiphoton ionization becomes the dominant ionization mechanism in

the femtosecond regime, since the pulse duration is shorter than an average collision time.

Figure 2(c) shows how ultrafast plasma creation blue shifts the spectrum of 100-fsec pulses. These spectra were collected after the $f/2$ focus and averaged over 100 shots by an optical multichannel analyzer as focal intensity was varied with neutral-density filters. At intensities below threshold [back spectrum in Fig. 2(c)] the spectrum of the focused pulse is centered at 626 nm, with a FWHM of 11 nm, and is identical to that of the unfocused pulse. Little change occurs below breakdown [arrow in Fig. 2(c)], indicating that nonlinear optical interaction with air is weak under our conditions. Above threshold, however, we observe a pronounced blue shift in the entire pulse spectrum, which increases up to a focal intensity of $\sim 2 \times 10^{15}$ W/cm^2, where the center wavelength reaches 615 nm. This shift is clearly correlated with the creation of a plasma. At higher intensities (up to 10^{16} W/cm^2), however, the blue shift saturates, leaving the pulse spectrum centered at 615 nm. The circles in Fig. 2(d) plot the center wavelength as a function of peak intensity. Weaker blue shifts can be observed with a longer focus if pressure is reduced enough (to <0.1 atm) to eliminate broadening caused by the third-order nonlinear susceptibility $\chi^{(3)}$ of the gas.[19] Although our blue shift is accompanied by 30% spectral broadening [Fig. 2(d)], we emphasize that, unlike the spectral broadening observed by others,[16,17] our spectra contain *only* blue-shifted components.

We attribute this blue shift to a negative refractive-index ramp caused by rapid creation of a plasma during the pulse. Blue shifts of similar origin have been observed with ~1-J CO_2 laser pulses under high-pressure gas-breakdown conditions.[20] With tightly focused femtosecond visible pulses, we observe a strong blue shift in atmospheric air with less than 1-mJ energy because of the ultrafast rate of plasma formation. Moreover, the temporal asymmetry of the index change is stronger than with longer pulses, since free electrons neither recombine nor escape from the focal region during a femtosecond pulse, thus further enhancing the blue shift.[19,20] By using a Drude model, the blue shift can be approximated as[20] $\Delta\lambda = (\lambda^3 e^2 L/2\pi mc^3)(dN/dt)$, where the interaction length $L \sim z_0 \sim 100\ \mu$m and the rate of change of electron density $dN/dt \sim \Delta N/\Delta t$, where ΔN is the plasma density created during the pulse and $\Delta t \sim 100$ fsec is the pulse duration. Thus the observed 11-nm blue shift requires that $\Delta N \sim 2.7 \times 10^{19}$ cm^{-3}, precisely the full atmospheric molecular density. Therefore at our highest intensities, the air must be completely singly ionized within the focal volume, causing the observed saturation of the blue shift. Index lensing in the plasma, manifested as an ~30% increase in beam divergence at our highest intensity, limits further expansion of the interaction region. We observe no filamentation. Yablonovitch[21] recently suggested a connection between such blue shifts and red-shifted photoelectron energies observed in recent femtosecond above-threshold-ionization experiments.[22]

In practical terms this blue shift provides a simple means of tuning millijoule femtosecond pulses over a limited wavelength range with virtually no loss in energy. While a wider tuning range is observed[23] at higher gas pressures, even the limited tuning range shown in Figs. 2(c) and 2(d) has a clear application in excimer pulse amplification. Since the fundamental pulse tunes through 616 nm, the second harmonic tunes through 308 nm and can thus be centered precisely on the XeCl gain curve. We have generated 308-nm pulses with good spectral and energy stability at ~5% conversion efficiency, comparable with that achievable with unshifted pulses.

This research was supported by the Robert A. Welch Foundation (grant F-1038), the Joint Services Electronics Program (contract F49620-86-C-0045), a National Science Foundation Presidential Young Investigator Award (grant DMR-8858388), and an IBM Faculty Development Award. We thank F. P. Schäfer and P. B. Corkum for sharing copies of recent research with us before publication.

References

1. C. K. Rhodes, Science **229,** 1345 (1985).
2. J. Glownia, J. Misewich, and P. P. Sorokin, J. Opt. Soc. Am. B **4,** 1061 (1987).
3. R. L. Fork, C. V. Shank, and R. Yen, Appl. Phys. Lett. **41,** 223 (1982).
4. M. M. Murnane and R. W. Falcone, J. Opt. Soc. Am. B **5,** 1575 (1988).
5. C. Rolland and P. Corkum, Opt. Commun. **59,** 64 (1986).
6. S. Szatmari, F. P. Schäfer, E. Muller-Horsche, and W. Muckenheim, in *Digest of International Quantum Electronics Conference* (Optical Society of America, Washington, D.C., 1987), paper PD20.
7. T. Turner, M. Chatelet, D. S. Moore, and S. C. Schmidt, Opt. Lett. **11,** 357 (1986).
8. W. H. Knox, IEEE J. Quantum Electron. **QE-24,** 388 (1988).
9. W. H. Knox, M. C. Downer, R. L. Fork, and C. V. Shank, Opt. Lett. **9,** 552 (1984).
10. F. P. Schaefer, Appl. Phys. B **39,** 1 (1986).
11. G. Kühnle, G. Marowsky, and G. A. Reider, Appl. Opt. (to be published).
12. W. M. Wood, G. W. Burdick, and M. C. Downer, in *Technical Digest of Conference on Lasers and Electro-Optics* (Optical Society of America, Washington, D.C., 1988), p. 116.
13. D. S. Bethune, Appl. Opt. **20,** 1897 (1981).
14. J. D. Kafka and T. Baer, Opt. Lett. **12,** 401 (1987).
15. J. M. Liu, Opt. Lett. **7,** 196 (1982).
16. P. B. Corkum, C. Rolland, and T. Srinivasan-Rao, Phys. Rev. Lett. **57,** 2268 (1986); J. H. Glownia, J. Misewich, and P. P. Sorokin, J. Opt. Soc. Am. B **3,** 1573 (1986).
17. D. Kühlke, U. Herpers, and D. von der Linde, Opt. Commun. **63,** 275 (1987).
18. C. G. Morgan, Rep. Prog. Phys. **38,** 621 (1975).
19. P. B. Corkum and C. Rolland, in *NATO ASI Series—Physics B,* A. Borndrawk, ed. (to be published).
20. E. Yablonovitch, Phys. Rev. Lett. **32,** 1101 (1974); Phys. Rev. A **10,** 1888 (1974); P. B. Corkum, IEEE J. Quantum Electron. **QE-21,** 216 (1985).
21. E. Yablonovitch, Phys. Rev. Lett. **60,** 795 (1988).
22. R. R. Freeman, P. H. Bucksbaum, H. Milchberg, S. Darack, D. Schumacher, and M. E. Geusic, Phys. Rev. Lett. **59,** 1092 (1987).
23. M. C. Downer, G. Focht, D. H. Reitze, W. M. Wood, and T. R. Zhang, *Ultrafast Phenomena VI* (Springer-Verlag, Heidelberg, to be published).